Arabian Journal of Chemistry (2018) **xxx**, xxx–xxx

King Saud University

Arabian Journal of Chemistry

www.ksu.edu.sa
www.sciencedirect.com

ORIGINAL ARTICLE

Unveiling interactions between DNA and cytotoxic 2-arylpiperidinyl-1,4-naphthoquinone derivatives: A combined electrochemical and computational study

Christian Espinosa-Bustos [a,*], Camila Canales [b], Galo Ramírez [b], Pablo Jaque [c,d], Cristian O. Salas [a,d,*]

[a] *Departmento de Química Orgánica, Facultad de Química, Pontificia Universidad Católica de Chile, Avenida Vicuña Mackenna, 4860, Santiago, 702843, Chile*
[b] *Departmento de Química Inorgánica, Facultad de Química, Pontificia Universidad Católica de Chile*
[c] *Departamento de Ciencias Químicas, Facultad de Ciencias Exactas, Universidad Andres Bello, Av. República 275, Santiago, Chile*
[d] *Nucleus Millennium of Chemical Processes and Catalysis, Faculty of Chemistry, Pontificia Universidad Católica de Chile, Avenida Vicuña Mackenna, 4860, Santiago, 702843, Chile*

Received 3 January 2018; accepted 15 April 2018

KEYWORDS

Naphthoquinone derivatives;
Cytotoxicity;
DNA interaction;
Electrochemistry;
Computational study

Abstract Three 2-arylpiperidinyl-1,4-naphthoquinone derivatives were synthesized and evaluated *in vitro* to determine their cytotoxicity on cancer and normal cell lines. In order to establish their possible action mechanism, the electrochemical behaviour of these quinones was examined using cyclic voltammetry (CV) as technique by using a three-electrode setup: a glassy carbon, Ag/AgCl (in 3 M KCl), and platinum wire as working, reference, and counter electrodes, respectively. Kinetic studies were done to determine the control of the reduction reaction and the number of transferred electrons in the process. Furthermore, the addition of dsDNA to the quinone solutions allowed for the observation of an interaction between each quinone and dsDNA as the current-peaks became lower in presence of dsDNA. Otherwise, motivated to support the aforementioned results, electronic structure calculations at the TPSS-D3/6-31 + G(d,p) level of theory were carried out in order to find the most favourable noncovalently bonded complexes between quinones and DNA. Noncovalent complexes formed between DNA and 2-arylpiperidinyl-1,4-naphthoquinones and stabilized by π-stacking interactions along with the well-known hydrogen-bonded complexes were found, with

* Corresponding authors at: Departmento de Química Orgánica, Facultad de Química, Pontificia Universidad Católica de Chile, Avenida Vicuña Mackenna, 4860, Santiago, 702843, Chile.
E-mail addresses: ccespino@uc.cl (C. Espinosa-Bustos), cosalas@uc.cl (C.O. Salas).

Peer review under responsibility of King Saud University.

Production and hosting by Elsevier

https://doi.org/10.1016/j.arabjc.2018.04.008

the former being more stable than the latter. These results suggest that the intercalation of these quinone derivatives in DNA is the most likely action mechanism.

1. Introduction

Quinones are compounds widely found in nature that possess well-known biological properties. Therefore, their study represents a privileged interest for the pharmaceutical industry (Martínez and Benito 2005; Salas et al., 2011; Kumagai et al., 2012; Tandon and Kumar 2013; Klotz et al., 2014; Naujorks et al., 2015). In this sense, the most significant and largely distributed family of quinones are those based on the 1,4-naphthoquinone, which has shown a remarkable variety of therapeutic activities, antibacterial (Tandon et al., 2006; Ibis et al. 2011), antiviral (Tandon et al., 2006), antifungal (Tandon et al. 2009; Ferreira Mdo et al. 2014), anti-*T Cruzi* (Cuellar et al. 2003; Vazquez et al. 2015) and anticancer properties (Mallavadhani et al., 2014; Hong et al., 2015; Wellington 2015). The activity exhibited by 1,4-naphthoquinone derivatives makes them very attractive as building blocks to guide the synthesis of new, promising anticancer drugs. Additionally, several action mechanisms have been postulated, including their interaction with topoisomerases, their ability to generate semiquinone radical anions and reactive oxygen species (ROS) as well as their intercalation in DNA (Asche 2005; Smith et al., 2014; Hong et al. 2015; Wellington 2015). Among the group of naphthoquinones with known antitumor activity, the fragment 2-aminonaphthoquinone stands out. This compound is included in naturally occurring compounds such as griffithazanone A and calothrixin A/B as well synthetic analogues, such as 2-piperazinyl-naphthoquinone (Fig. 1) (Chen et al., 2003; Zhou et al., 2009; Tip-pyang et al., 2010).

It has been noted that the interaction of quinones with DNA is one of the most important issues in drug discovery. Overall, there are two modes of interaction: covalent and non-covalent, with the latter being the most common and selective for DNA via molecular recognition between the macromolecule and target systems. Many experimental methods have been employed to reveal the DNA-drug interactions, e.g., UV–Vis (Maleev et al. 2003), IR and Raman (Stanicova et al., 1999), fluorescence spectroscopies (Ni et al., 2011), capillary electrophoresis (Ryvolova et al., 2012) and voltammetric techniques (Radi et al., 2005, 2014). By noting the change in the shape and/or shift of the electrochemical signals, the latter techniques have been successful used to identify DNA-drug interactions. Quinone electroactivity has additionally allowed for the development of several electrochemical-based DNA sensors (Erdem and Ozsoz 2002; Reisberg et al., 2008; Hernandez et al., 2016). This feature is supported by the fact that quinone/hydroquinone couples are the most typical examples of organic redox systems and its electrochemical behaviour is essential in determining electron transfer - proton transfer mechanisms in reactions that are important in chemistry and biology and that provide valuable information regarding molecular structure (Hong and Park 2001; Guin et al., 2011).

Given that one of the possible action mechanisms for quinone derivatives is their interaction with DNA and considering that this behaviour can be studied using an electrochemical method, the aim of this paper is to offer a suitable and reliable method for evaluating and revealing drug–DNA interactions on cancer cell lines. To achieve this goal, we first synthesized and characterized three new 2-arylpiperidinyl-naphthoquinone derivatives, including 2-amino-1,4-naphthoquinones, as a training set. Both the cytotoxicity and selectivity of the compounds were evaluated using four cancer cell lines and Vero cells in order to determine their potential antitumor effects. Second, we studied the interaction of these quinones with double-stranded DNA (dsDNA) using cyclic voltammetry with the goal exploring their action mechanism. Finally, we carried out a computational study based on density functional theory calculations in order to support our results. As a result, different noncovalently bonded complexes of 2-arylpiperidi nyl-naphthoquinones derivatives with four canonical nucleobases and two Watson-Crick base pairs were found.

2. Results and discussion

2.1. Chemistry

The synthesis of the new 2-arylpiperidinyl-1,4-naphtoquinone (**3a-c**) compounds was carried out in a single step shown in Scheme 1. A convenient approach based on the classic method of nucleophilic substitution reaction between different haloquinones **1a-c** and phenylpiperidine **2** was performed at room temperature using ethanol as solvent (Sieveking et al. 2014), and the formation of **3a-c** proceeded in the range of 49–60%

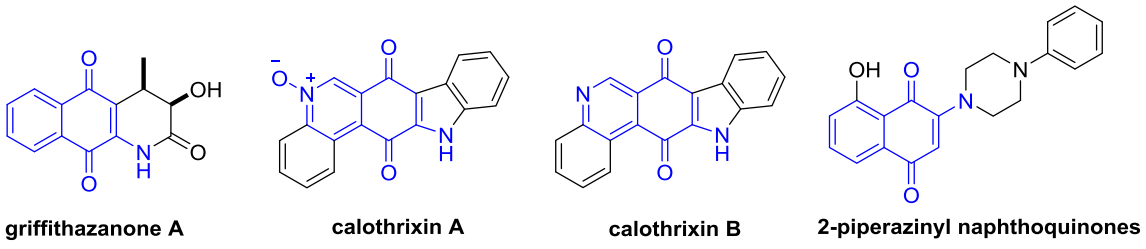

Fig. 1 2-amino-1,4-napthoquinone-type compounds with anticancer activities.

Please cite this article in press as: Espinosa-Bustos, C. et al., Unveiling interactions between DNA and cytotoxic 2-arylpiperidinyl-1,4-naphthoquinone derivatives: A combined electrochemical and computational study. Arabian Journal of Chemistry (2018), https://doi.org/10.1016/j.arabjc.2018.04.008

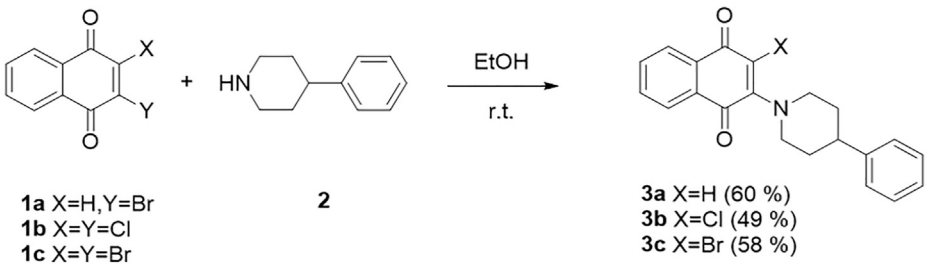

Scheme 1 Synthesis of the target compounds **3a–c**.

yield. The structures of the new compounds were confirmed using their proper spectral characterization (IR, ^{1}H NMR, ^{13}C NMR and HRMS).

2.2. Cytotoxic studies

The *In vitro* antitumor activity of compounds **3a–c** was assayed in order to reveal their potential cytotoxic effects on the following cancer cell lines HL-60, HeLa, HCT116 and H1975, and Vero cells. A colorimetric assay was set up to calculate the IC_{50} values, which represent the drug concentration required for 50% inhibition *in vitro* after 72 h of continuous exposure to these new compounds. Four serial dilutions (from 0.1 to 50 μM) for each sample were evaluated in triplicate in three independent experiments.

Table 1 shows the IC_{50} values for cytotoxicity of compounds **3a-c** on four cancer cell lines and Vero cell line. In general, 2-arylpiperidinyl-1,4-naphtoquinone derivatives activity was quite homogenous (IC_{50} range of 30–7.0 μM on cancer cell lines), which is due to the similar chemical structures of these compounds. However, the best results for both cytotoxicity activity and selectivity were observed on the HCT116 cell line. In this case, all target compounds presented IC_{50} values <11.0 μM and were thus more active than the reference anticancer drug on this cell line. In addition, these derivatives exhibited a higher selective index (SI) with values >4.6 (see Table 1) than etoposide. The IC_{50} values were shown to be discrete in other cell lines. All **3a-c** compounds showed lower cytotoxicity and selectivity than the reference drug for the HL-60 cell line. While these compounds revealed a moderate cytotoxicity compared to etoposide in H1975, except for compound **3a** (IC_{50} value = 10.9 μM), the compounds **3b** and **3c** were more active (IC_{50} values = 12.8 and 11.6 μM, respectively) as well as more selective (SI values = 3.9 and 4.3, respectively) than etoposide in the HeLa cancer cell line. It is important to note that the SI values also indicated a lower toxicity to normal cells, which is an essential requirement for new anticancer agents. Our results are in accordance with the protocols of the National Cancer Institute (NCI) (NCI 2014), where compounds with IC_{50} values <10 μM or 15 μM can be considered potentially active.

2.3. Voltammetric analyses

Unlike the voltammetric response that the quinones have in non-aqueous media, these show one main cathodic and one main anodic peak current (Fig. 2), which can be attributed to the behaviour of these molecules in this media that implies that their electrochemical reduction from quinone Q into hydroquinone QH_2 proceeds through the transfer of two electrons, where redox processes are coupled and occur at nearly the same potential. Then, the overall reaction is shown by the Eq. (2):

$$Q + 2H^{+} + 2e^{-} \rightarrow QH_2 \quad (1)$$

This electrochemical behaviour can advance either in presence or in absence of H^{+}, depending on the acidity of environment (Guin et al., 2008,2011).

2.3.1. Voltammetric responses and kinetic analyses

Fig. 2 shows the voltammetric response of the new 2-arylpiperidinyl-1,4-naphtoquinones (**3a-c**) in the DMSO-PBS (1:9 v/v,

Table 1 *In vitro* cytotoxicity of compounds **3a–c** on cancer cell lines and Vero cells.

	IC_{50} (μM)[a]								
	HL-60[b]	SI[c]	HeLa[d]	SI	HCT116[e]	SI	H1975[f]	SI	Vero[g]
3a	14.4 ± 3.5	3.5	30.2 ± 5.2	1.6	10.9 ± 1.1	4.6	10.9 ± 1.2	4.6	> 50 μM
3b	19.9 ± 4.3	2.5	12.8 ± 4.1	3.9	9.3 ± 1.1	5.4	23.1 ± 4.9	2.2	> 50 μM
3c	13.5 ± 2.2	3.7	11.6 ± 3.8	4.3	6.9 ± 2.3	7.2	17.8 ± 4.2	2.8	> 50 μM
Etoposide	3.0 ± 1.1	16.7	21.2 ± 3.8	2.4	22.0 ± 4.1	2.3	8.0 ± 0.3	6.3	> 50 μM

[a] IC_{50} values were determined in three independent experiments for triplicate in the range of 0.05–50 μM.
[b] Human promyelocytic leukemia cells.
[c] Selectivity index (SI) = IC_{50} value of pure compound in a normal cell line/IC_{50} value of the same pure compound in cancer cell line.
[d] Human cervix adenocarcinoma cells.
[e] Human colorectal carcinoma cells.
[f] Human lung cancer cells.
[g] Green monkey normal kidney cells.

Please cite this article in press as: Espinosa-Bustos, C. et al., Unveiling interactions between DNA and cytotoxic 2-arylpiperidinyl-1,4-naphthoquinone derivatives: A combined electrochemical and computational study. Arabian Journal of Chemistry (2018), https://doi.org/10.1016/j.arabjc.2018.04.008

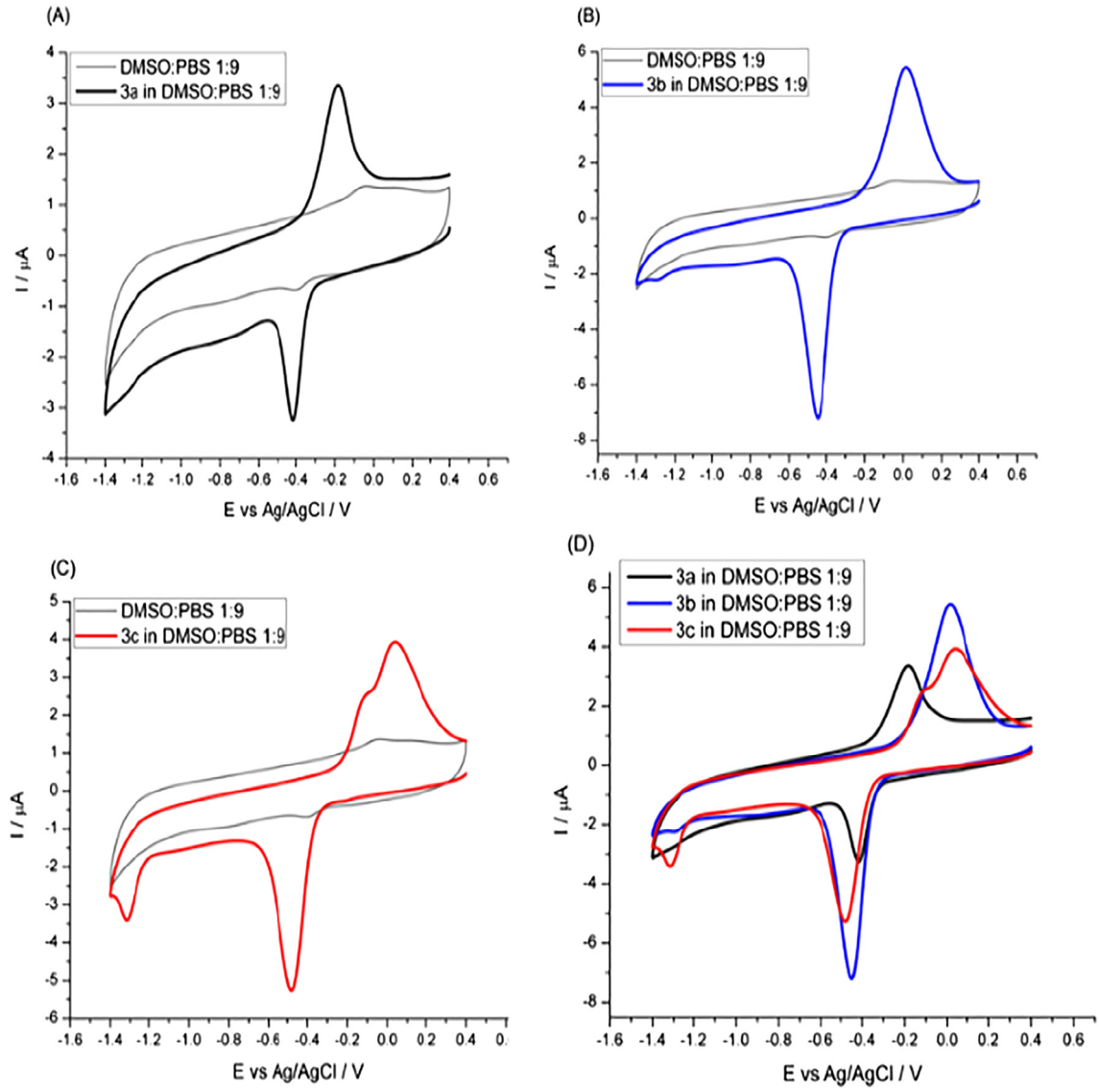

Fig. 2 Voltammetric profiles of 50 µM of (A) **3a**, (B) **3b**, (C) **3c** dissolved in DMSO:PBS (1:9 v/v, pH 7.2, 0.066 M, saturated in Ar) and the superposition of all profiles (D). Scan rate, $\nu = 100\ mVs^{-1}$.

pH 7.2, 0.066 M) solution. The three quinones presented a single cathodic wave in the range of −0.4 V to −0.5 V, referred to Ag/AgCl electrode, which present quasi-reversible responses (Bard, 2000). In this sense, it is observed that quinone 3c is the less reversible one, since the separation of its current responses (anodic/cathodic) is more significant than the responses that quinones 3b and 3a show. The cathodic peak potential shifted towards a more negative potential as the substituent X moved from H to Br by 70 mV (see Table 2). This means that quinone **3c** is less easily reduced than **3a**. A striking shoulder was found near the main anodic peak in the voltammetric contour of **3c**. This may be related to the weak cathodic peak located at −1.3 V (vs. Ag/AgCl), which would then suggest that a different mechanism may be operating in the electrochemical reduction for this quinone. A new voltammogram was recorded until −0.9 V and confirmed the anodic response corresponding to the cathodic wave at −1.3 V disappearing in the reverse scan. In this sense, this could mean that the second reduction peak of **3c** is due to the presence of a persistent radical anion in the vicinity of the electrode surface (Bouffier et al., 2012). At this point, the voltammetric shape of **3c** resembled those observed for quinones in non-aqueous solvents as DMSO or DMF. In those cases, the first cathodic peak was attributed to the reduction of C═O next to the piperidine ring as the halogen (Br) tends to attract the electronic density, leaving this fraction of the molecule devoid of electrons and making it an easier site to reduce other than the C═O fraction located next to the bromide. Then, the regeneration of this last C═O from the ─OH specie in the

Table 2 Ep_c, $Ep_{c/2}$ and number of electrons (n) involved in the reduction reaction of quinones.

Compound	Ep_c (V)	$Ep_{c/2}$ (V)	n
3a	−0.41	−0.37	2 (2.3)
3b	−0.45	−0.40	2 (1.8)
3c	−0.48	−0.41	1 (1.2)

Please cite this article in press as: Espinosa-Bustos, C. et al., Unveiling interactions between DNA and cytotoxic 2-arylpiperidinyl-1,4-naphthoquinone derivatives: A combined electrochemical and computational study. Arabian Journal of Chemistry (2018), https://doi.org/10.1016/j.arabjc.2018.04.008

reverse scan was more easily obtained than the first one whose proximity to the piperidine resulted in a less reversible wave.

In order to get more information concerning the mechanism of the electrochemical reduction reaction of each quinone, the dependence of the voltammetric response towards the variation of the scan rate ν was studied as recommended by the Randles-Sevcik equation. Fig. 3 displays the results obtained. As can be seen, the plots between log Ip *versus* log ν show a linear behaviour with a slope of 0.9, 1 and 1 for **3a**, **3b** and **3c**, respectively. This implies that all systems are

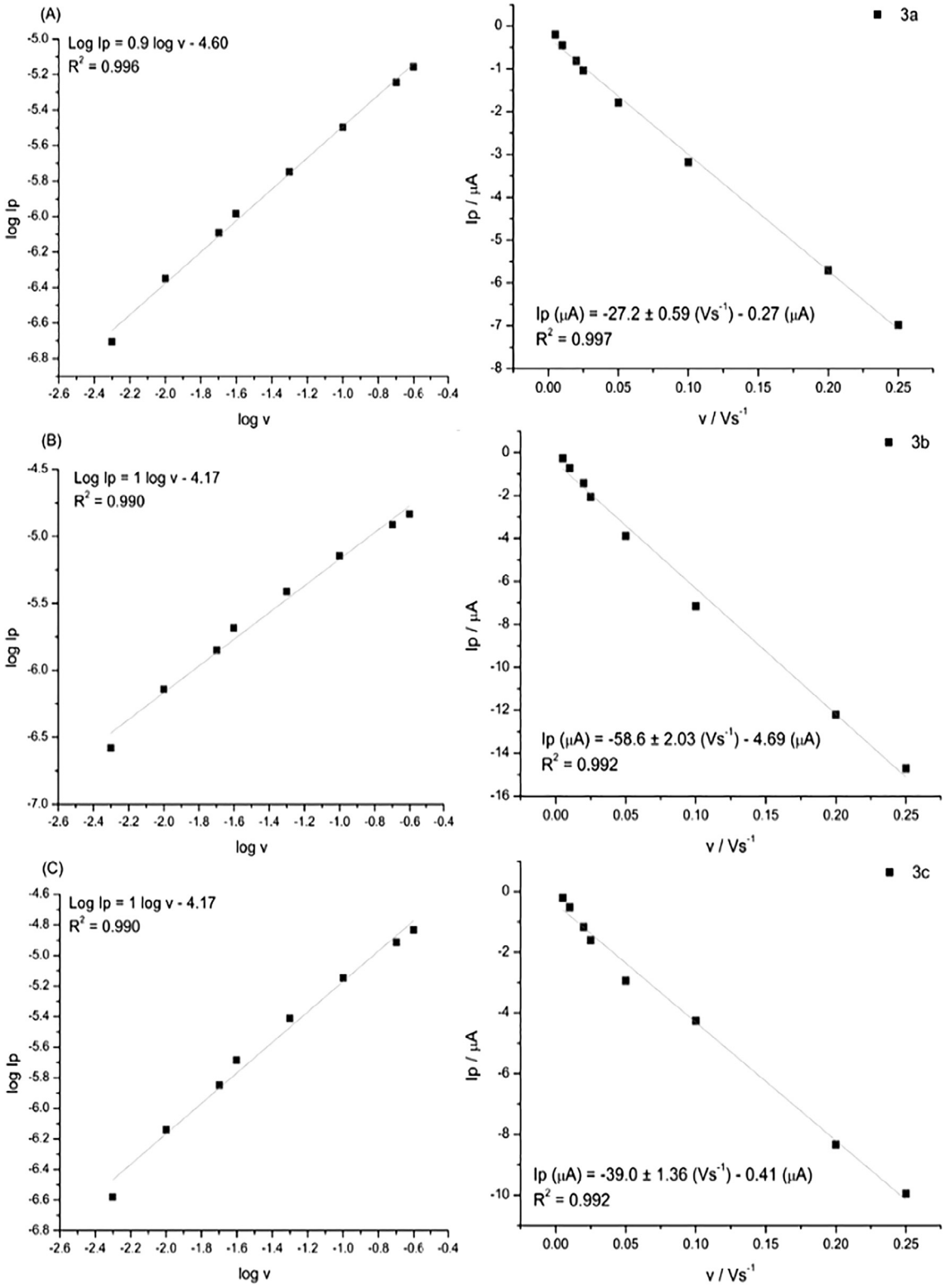

Fig. 3 Kinetic analysis of the electroreduction of compounds **3a–c**: log Ip *versus* log ν plots (left panels) and Ip *versus* scan rate (ν) plots (right panels).

adsorption-controlled rather than diffusion-controlled processes. Subsequently, a plot of Ip against the scan rate (ν) gave a correlation coefficient (R^2) close to the unity, reinforcing the findings that the process is controlled by adsorption (Bard 2000). All these studies were done considering the cathodic peak current.

These results are consistent with other previous works (Chaney and Baldwin 1982; Kano et al., 1984), where, under these experimental conditions, the electrochemical reaction is purely adsorption-controlled with negligible diffusion control. Then, considering that glassy carbon electrodes may have oxidized sites, the functional groups, such as —CHO, —COOH and —OH, among others (Tanaka and Aramata 1997), can strongly interact with quinones, thus producing adsorption at the electrode surface. In this kind of reaction, the number of electrons involved in the reduction may be calculated using the Eq. (3) (He et al., 1990), and should result in 2 electrons. Table 2 summarizes the Ep_c and $Ep_{c/2}$ that are needed to calculate the number of electrons involved in each reaction.

$$\left|E_{pc} - \frac{E_{pc}}{2}\right| = \frac{90.6}{n} \quad (2)$$

Based on this information, the reduction mechanism of an electrochemical reaction for each quinone is shown in Fig. 4. This mechanism is known as the ECEC or EHEH mechanism (E = electrochemical step, C = chemical step, H = proton transfer), which means it is composed of two rounds of electron-transfer coupled with proton acceptance (chemical reaction).

For compounds **3a** and **3b**, both of the aforementioned redox processes are strongly coupled and take place nearly at the same potential. Consequently, just one cathodic peak and one anodic peak is observed. However, for compound **3c**, two cathodic peaks are observed, which explains why the number of transferred electrons on the first reduction peak was close to one. The second electron-transfer did not proceed until −1.3 V, which can be attributed to the effect of the substituent (Br) that may difficult the reduction of carbonyl functional group, as it was aforementioned. This effect can also be observed in the quinone 3b, but the intensity of the cathodic peak at −1.2 V is lower, since the effect of the substituent in this case (Cl) is less significant in comparison to the one showed by the Br. Then, a higher fraction of the quinone total concentration is being reduced at potentials near to −0.4 V. In this way, the calculated transferred electrons is 2 for the quinone 3a as well as for the quinone 3b, while quinone 3c tends to transfer 1 electron, since a significant part of the total concentration of the quinone is not totally reduced.

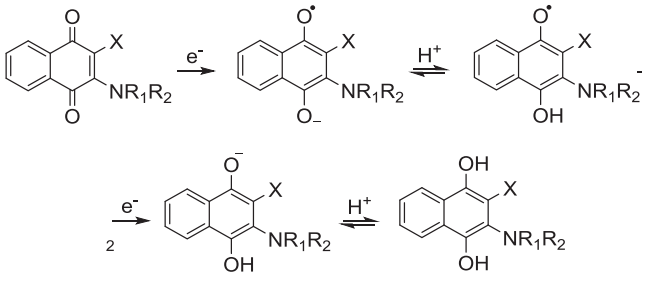

Fig. 4 Mechanism for the electrochemical reduction of **3a–c** derivatives (X = H, Cl, Br).

2.3.2. Interaction between 2-Arylpiperidinyl-1,4-naphthoquinones with dsDNA

Cyclic voltammograms were also obtained for each solution prepared with each compound **3a–c** + dsDNA and previously incubated at 37 °C for 45 min. It was noted that during incubation, the coloured solutions became transparent, unveiling an interaction between the 2-arylpiperidinyl-1,4-naphthoquinones and dsDNA, a process which may be driven by either covalent or noncovalent interactions.

Fig. 5 displays the voltammograms for **3a–c** + dsDNA solutions at different dsDNA concentrations. It was observed that, in all cases, the current-peaks corresponding to the redox activity of quinone severely decays. As more dsDNA is added to the solution, the current-peaks decrease until they are imperceptible. This effect indirectly demonstrates that the quinone derivatives interact with the macromolecule, consequently resulting in smaller concentrations of quinone available to be electrochemically reduced. Thus, the concomitant current-peaks are related to the amount of available quinone in the bulk solution. Additionally, it was also observed that, as more dsDNA is added to the solution, the onset reduction overpotential shifts slightly to less negative values in all cases. This means that the available quinone is more easily reduced than in absence of the dsDNA macromolecule. Again, it is interesting to observe the effect on the second cathodic peak of compound **3c**, where the current-peaks was found to increase as the concentration of dsDNA also increased.

2.4. Quantum chemical calculations

To support the observations discussed above, some quantum chemical calculations based on the TPSS-D3/6-31 + G(d,p) level of theory were performed. The intention of performing these calculations was to search the intermolecular complexes between the new 2-arylpiperidinyl-1,4-naphthoquinones (**3a–c**) and dsDNA, with the latter being modelled using single canonical nucleobases and two planar Watson-Crick base pairs. Two types of noncovalent bound complexes were fully optimized, which are mainly stabilized by hydrogen bonding (labelled as C1) and π-stacking (labelled as C2) interactions. The stability was calculated using Eq. (1), which describes the overall energy change, ΔE, due to the formation of the respective complexes. The more negative the ΔE value, the more stable the noncovalently bonded complex (or more favourable binding mode).

2.4.1. Intermolecular complexes formed between quinones and single nucleobases

The new 2-arylpiperidinyl-1,4-naphthoquinones (**3a–c**) and each canonical nucleobase, i.e. A, C, T and G can form noncovalent complexes that are mainly stabilized by hydrogen-bonding (C1) and π-stacking (C2) interactions. The former can be further divided into two subcategories: those forming an H-bond with the oxygen atom belonging to the carbonyl group adjacent to the X substituent (C1) and those with the oxygen atom belonging to the carbonyl group close to arylpiperidinyl group (C1′). The computed stability of the respective complex is shown in Table 3.

At first glance, it was observed that the new quinones bind more favourably to nucleobases through π-stacking

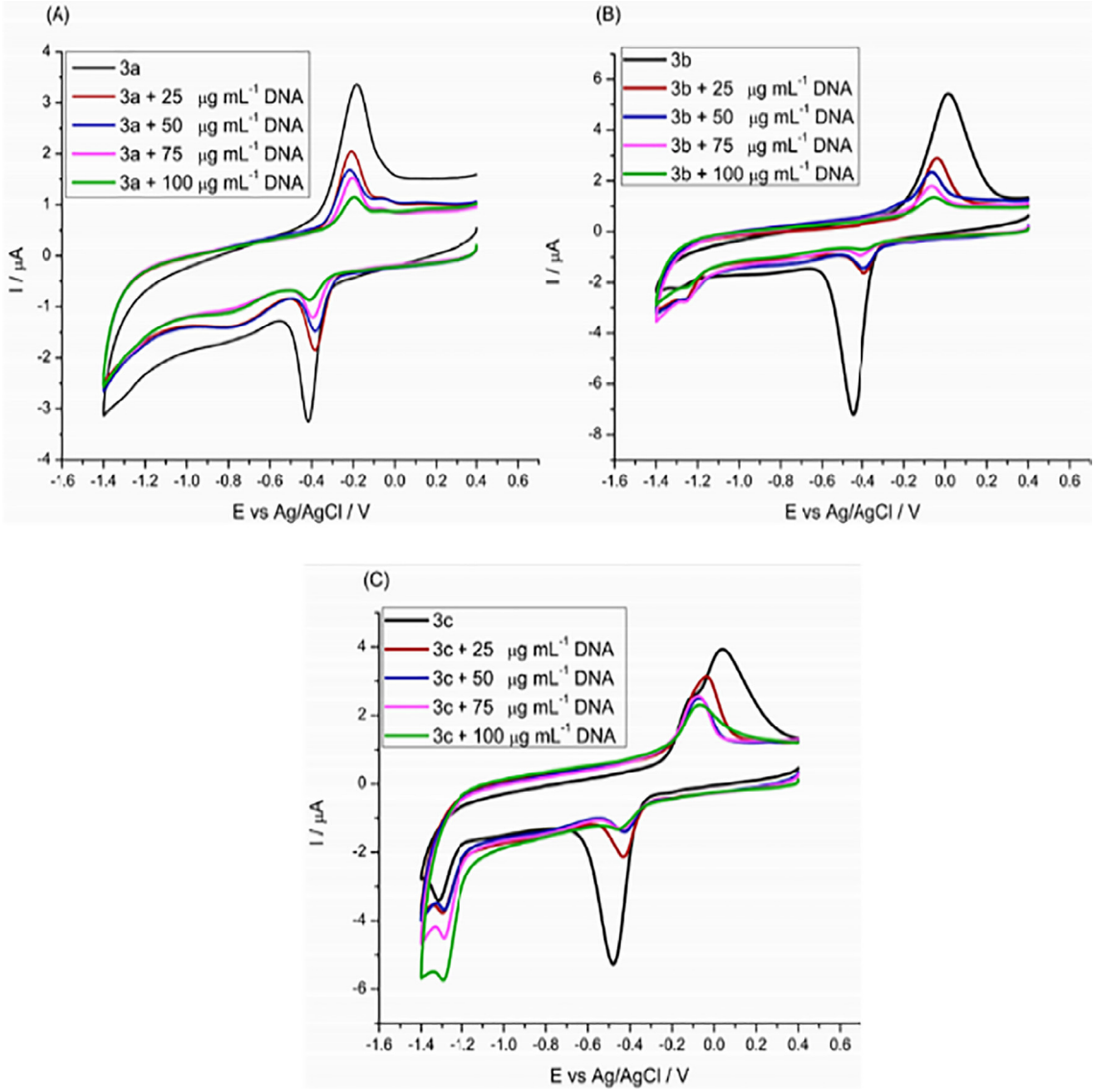

Fig. 5 CV of 50 μM of 3a-c dissolved in DMSO:PBS 1:9 (pH 7.2, 0.066 M) in the absence and presence of dsDNA. Scan rate, v = 100 mVs^{-1}, saturated in Ar.

interactions than through hydrogen-bonding interactions, by about 4.0 kcal/mol on average. The π- stacking interactions include both the sandwich (for A, T, and G) and T-shaped (for C) orientations. However, these can be assisted by H-bond interactions in some cases, as shown in Fig. 6, since their H···O and H···N distances are shorter than the sum of the van der Waals radii. It was noted that the strength of stacking interactions (assisted by hydrogen bonding) for the single nucleobase increases for A or T followed by G or C depending the quinone. Additionally, the oxygen atom of the C═O group adjacent to X leads to a stronger H-bond than the oxygen atom close to the arylpiperidinyl group, except for T.

2.4.2. Intermolecular complexes formed between quinones and Watson-Crick base pairs

The noncovalent complexes formed by the new 2-arylpiperidinyl-1,4-naphthoquinones (**3a–c**) and the two planar Watson-Crick base pairs stabilized by the H-bond (labelled as C1) and π-stacking (labelled C2) interactions were also fully optimized. Their corresponding stability is reported in Table 4.

Again, it can be observed that the complexes stabilized by π-stacking are far more favourable than those stabilized by H-bond interactions, meaning that the compound **3c** is more stabilized than **3a** and **3b** with both Watson-Crick base pairs. Some of these complexes can be found in Fig. 7 where it can be also noted that H···O and H···N interactions assisted the formation of the noncovalently bound complexes. Owing to the weakness and strength of the H-bond between A---T and G---C, respectively, the formation of hydrogen-bonding interactions with the new quinones is slightly stable and unfeasible from a thermodynamic perspective for both the former and the latter. Consequently, the most attainable interaction mode is through π-stacking interactions that are assisted by some H-bonds.

In light of the above results, the most plausible action mechanism of the interaction between the new cytotoxic 2-aryl piperidinyl-1,4-naphtoquinones with dsDNA is the intercalation of DNA.

Please cite this article in press as: Espinosa-Bustos, C. et al., Unveiling interactions between DNA and cytotoxic 2-arylpiperidinyl-1,4-naphthoquinone derivatives: A combined electrochemical and computational study. Arabian Journal of Chemistry (2018), https://doi.org/10.1016/j.arabjc.2018.04.008

Table 3 Computed stability of the noncovalently bonded complexes between quinones (**3a–c**) and canonical nucleobases at TPPS-D3/6-31 + G(d,p) level. All values are given in kcal/mol.

Complex	ΔE		
	C1	C1′	C2
3a···**A**	−8.79	−7.93	−12.38
3a···**T**	−9.28	−10.11	−13.10
3a···**C**	−12.95	−11.01	−17.24
3a···**G**	−−16.10	−13.38	−15.46
3b···**A**	−8.63	−7.92	−13.52
3b···**T**	−8.70	−10.13	−11.58
3b···**C**	−13.05	−11.29	−16.96
3b···**G**	−16.26	−13.08	−18.07
3c···**A**	−9.25	−8.05	−17.10
3c···**T**	−9.30	−10.58	−15.50
3c···**C**	−13.77	−11.68	−20.87
3c···**G**	−17.01	−13.29	−19.13

Table 4 Computed stability of the noncovalently bonded complexes between quinones (3a-c) and Watson-Crick base pairs at TPPS-D3/6-31 + G(d,p) level. All values are given in kcal/mol.

Complex	ΔE	
	C1	C2
3a···AT	−1.76	−8.89
3b···AT	−1.66	−8.35
3c···AT	−0.10	−17.19
3a···GC	10.34	−2.60
3b···GC	10.75	−3.11
3c···GC	10.08	−11.11

3. Conclusions

The electrochemical behaviour of three new cytotoxic 2-arylpi peridinyl-1,4-naphtoquinones was examined to understand a possible action mechanism in some cancer cell lines. At this point, the electrochemical/kinetic measurements showed that the reduction reaction of each quinone was adsorption-controlled and 2, 2 and 1 electrons are transferred in the reduction process of quinones **3a**, **3b** and **3c**, respectively. The reduction mechanism of these quinones ranged from reversible to quasi-irreversible as the X substituent changed from H to Br passing by Cl. When these compounds were incubated with dsDNA solutions, a decrease in their respective current-peaks was observed thus unveiling a significant interaction between the cytotoxic quinones with DNA. In order to confirm the interaction between quinones and dsDNA, electronic structure calculations based on the TPSS-D3/6-31 + G(d,p) level of theory were carried out. These revealed that the three quinones can be stabilized by single canonical nucleobases and Watson-Crick base pairs forming intermolecular complexes bound by two noncovalent interactions, i.e. π-stacking (assisted by some H-bonds) interactions and hydrogen-bonding, with the former being more stable than the latter. This suggests that intercalation of the new cytotoxic quinones in DNA is the main action mechanism. This combined electrochemical and computational study allows us to explain the effect of the new quinones synthesized on cancer cell lines. Additionally, the present approach could be seen as a suitable and reliable method for future studies in biological systems as they offer several benefits, such as low cost, fast, high-sensitivity, and simple design. These are high-quality analytical options for evaluating and revealing drug–DNA interactions. Moreover, the importance of this work is to extend these studies to known DNA sequences, such as some oligopeptides. These works will be carried out in the near future.

4. Experimental

4.1. 1Materials and measurements

Uncorrected melting points were determined on a Kofler Thermogerate apparatus. Infrared spectra were recorded on a JASCO FT/IR-400 spectrophotometer. ^{1}H and ^{13}C nuclear magnetic resonance (NMR) spectra were recorded, unless

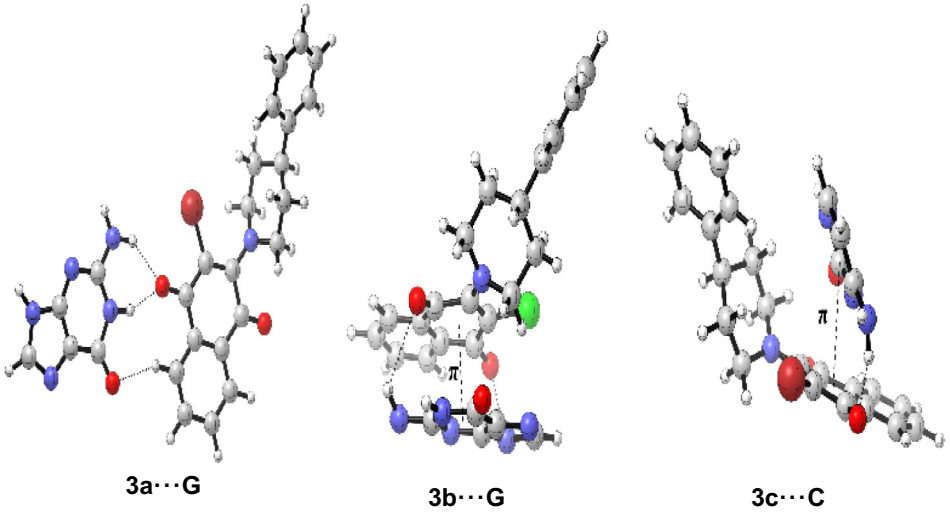

Fig. 6 Intermolecular complexes formed between **3a–c** and single nucleobases stabilized by hydrogen-bonding and π-stacking interactions.

Please cite this article in press as: Espinosa-Bustos, C. et al., Unveiling interactions between DNA and cytotoxic 2-arylpiperidinyl-1,4-naphthoquinone derivatives: A combined electrochemical and computational study. Arabian Journal of Chemistry (2018), https://doi.org/10.1016/j.arabjc.2018.04.008

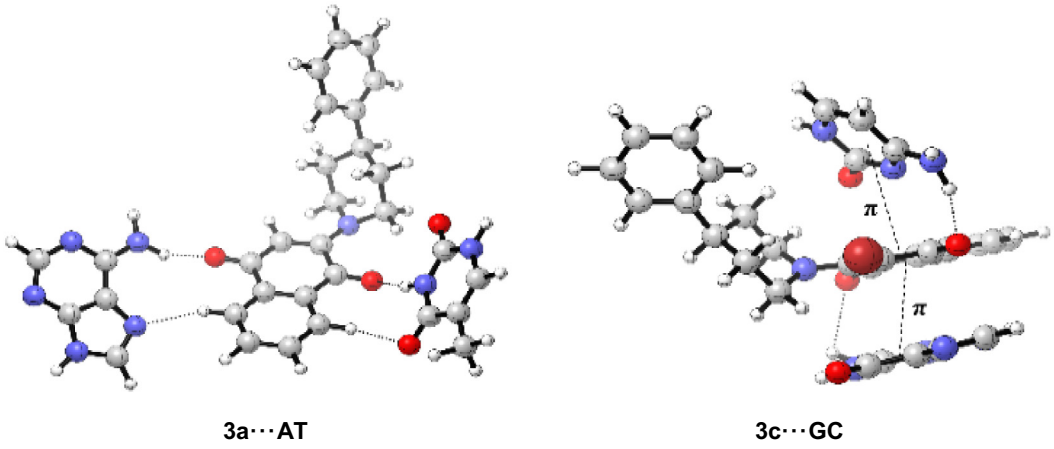

Fig. 7 Intermolecular complexes formed between **3a–c** and Watson-Crick base pairs stabilized by hydrogen-bonding and π-stacking interactions.

otherwise specified, on a Bruker AM-400 instrument using deuterochloroform or dimethylsulfoxide solutions containing tetramethylsilane as an internal standard. Mass spectra were obtained on a HP 5988A mass spectrometer. HRMS-ESI-MS experiments were done using a Thermo Scientific Exactive Plus Orbitrap spectrometer with a constant nebulizer temperature of 250 °C. The experiments were carried out in positive or negative ion mode, with a scan range of *m/z* 300.00-1510.40 with a resolution of 140.000, the samples were infused directly into the ESI source, via a syringe pump, at flow rates of 5 μL min^{-1}, through the instrument's injection valve. Thin layer chromatography (tlc) was performed using Merck GF-254 type 60 silica gel. Column chromatography was carried out using Merck type 9385 silica gel. The purity of the compounds was determined by tlc coupled to high-resolution mass spectrometry (HRMS).

4.2. General synthetic procedure and characterization of 2-arylpiperidinyl-quinones

A mixture of the suitable amount of each reactive, naphthoquinone (1 mmol), the required piperidine (1.2 mmol) and ethanol (20 mL) was stirring at room temperature for 6 h. Then the reaction mixture was evaporated under reduced pressure and the residue was separated by column chromatography using dichloromethane as eluent.

*4.2.1. 2-(4-Phenylpiperidin-1-yl)naphthalene-1,4-dione **3a***

Orange solid, yield 60%, mp 135–137 °C. ^{1}H NMR (400 MHz, $CDCl_3$) δ 8.04 (d, J = 7.5 Hz, 1H), 7.99 (d, J = 7.5 Hz, 1H), 7.68 (t, J = 7.4 Hz, 1H), 7.62 (t, J = 7.4 Hz, 1H), 7.31 (t, J = 7.5 Hz, 2H), 7.27–7.18 (m, 3H), 6.08 (s, 1H), 4.18 (d, J = 12.9 Hz, 2H), 3.12–3.01 (m, 2H), 2.90–2.72 (m, 1H), 2.03–1.85 (m, 4H). ^{13}C NMR (101 MHz, $CDCl_3$) δ 183.64, 183.32, 154.05, 145.01, 133.84, 132.94, 132.53, 132.37, 128.63, 126.77, 126.68, 126.59, 125.53, 111.25, 50.08, 42.55, 33.07. HRMS for ($C_{20}H_{18}N_2O_2$ [M]). Calcd: 318.1368 Found: 318.1493.

*4.2.2. 2-Chloro-3-(4-phenylpiperidin-1-yl)naphthalene-1,4-dione **3b***

Purple solid, yield 49%, mp 142–143 °C. ^{1}H NMR (400 MHz, $CDCl_3$) δ 8.08 (d, J = 7.3 Hz, 1H), 7.97 (d, J = 7.3 Hz, 1H), 7.69–7.58 (m, 2H), 7.33–7.09 (m, 5H), 3.90 (d, J = 12.9 Hz, 2H), 3.45–3.34 (m, 2H), 2.83–2.71 (m, 1H), 2.05–1.87 (m, 4H). ^{13}C NMR (101 MHz, $CDCl_3$) δ 182.08, 178.11, 150.69, 145.44, 134.04, 133.03, 131.73, 131.58, 128.58 (2C), 126.88, 126.85 (2C), 126.58, 126.48, 123.04, 52.55 (2C), 42.31, 34.24 (2C). HRMS for ($C_{20}H_{17}ClN_2O_2$ [M]). Calcd: 352.0979 Found: 352.1106.

*4.2.3. 2-Bromo-3-(4-phenylpiperidin-1-yl)naphthalene-1,4-dione **3c***

Purple solid, yield 58%, mp 187–189 °C. ^{1}H NMR (400 MHz, $CDCl_3$) δ 8.07 (d, J = 6.8 Hz, 1H), 7.97 (d, J = 6.8 Hz, 1H), 7.68–7.56 (m, 2H), 7.33–7.19 (m, 5H), 3.89 (d, J = 13.2 Hz, 2H), 3.45–3.35 (m, 2H), 2.82–2.74 (m, 1H), 2.06–1.93 (m, 4H). ^{13}C NMR (101 MHz, $CDCl_3$) δ 181.80, 178.22, 153.40, 145.48, 134.00, 133.03, 131.54, 131.44, 128.58 (2C), 126.96, 126.91, 126.86 (2C), 126.48, 116.98, 52.94 (2C), 42.25, 34.18 (2C). HRMS for ($C_{20}H_{17}BrN_2O_2$ [M]). Calcd: 396.0473 Found: 396.0603.

4.3. Biological activity

4.3.1. Cell lines culture

Cancer cell lines (H1975, HL60, HTC116, and Vero cells) were grown at 37 °C in humidified atmosphere of 5% CO_2 in RPMI 1640 culture medium supplemented with 10% foetal bovine serum and penicillin-streptomycin (100 UI/mL). HeLa cells were grown in EMEM culture medium, supplemented with 10% foetal bovine serum and penicillin-streptomycin (100 UI/mL).

4.3.2. Cytotoxicity study

Cytotoxicity assays were performed using the MTT reduction method as was previously described (Calderon-Arancibia et al. 2015). Briefly, cancer cell lines were plated in a flat-bottom 96-wells plate at 10.000 cells per well density. Then the cells were incubated in presence of the synthesized compounds at different concentrations (from 0.1 to 50 μM) in 200 μL of 10% foetal bovine serum-RPMI or EMEM culture medium at 37 °C for 72 h. 10 μL of MTT was added at a final concentration of 0.5 mg/mL, incubated at 37 °C for 4 h, and then solubilized with 10% sodium dodecyl sulfate (SDS) in 0.1 mM HCl and

Please cite this article in press as: Espinosa-Bustos, C. et al., Unveiling interactions between DNA and cytotoxic 2-arylpiperidinyl-1,4-naphthoquinone derivatives: A combined electrochemical and computational study. Arabian Journal of Chemistry (2018), https://doi.org/10.1016/j.arabjc.2018.04.008

incubated overnight at 37 °C. Formazan formation was measured at 570 nm in a multiwell reader (StatFax 4200, Awareness Technology, Inc. Palm City, FL, USA).

4.3.3. Statistical analysis

All data are expressed as means ± standard deviations from three independent experiments. IC_{50} (compound concentration necessary to decrease at 50% the MTT reduction) values, and the two-way analysis of variance (ANOVA) test were performed using Prism GraphPad 6.0f software (GraphPad Software Inc., San Diego, CA, USA) when it was required.

4.4. Electrochemistry

4.4.1. Reagents

KCl, dimethylsulfoxide (DMSO), Na_2HPO_4 and KH_2PO_4 were obtained from Merck as analytical grade reagents. Deionized water was obtained from a Millipore-Q system (18.2 MΩ cm). Argon (99.99% pure) gas was purchased from AGA, Chile. Phosphate buffer solution (PBS), consisting of $H_2PO_4^-/HPO_4^{2-}$ (0.066 M) was prepared at pH 7.2. Double-stranded deoxyribonucleic acid (dsDNA) from fish sperm was purchased from Sigma-Aldrich, Chile.

4.4.2. Cyclic voltammetry measurements

Cyclic voltammetry (CV) studies were performed on a CH Instrument 750D potentiostat galvanostat. The conventional three-electrode system included glassy carbon as working electrode, Ag/AgCl, 3 M KCl as reference electrode, and a platinum wire as counter electrode. The glassy carbon electrode was polished to a mirror finish on a felt pad using alumina slurries (0.3 μm), followed by sonication in DMSO/PBS (1:9 v/v) for 120 s to remove the excess of alumina, then washed in acetone and dried at room temperature. Finally, the electrode response was stabilized, by cycling the potential between 0.4 V and −1.4 V in DMSO/PBS (1:9 v/v, pH 7.2, 0.066 M, Ar atmosphere). Voltammetric measurements were thus done by cycling the potential between 0.4 V and −1.4 V in a 50 μM of each new synthesized quinone (**3a–c**) dissolved in DMSO/PBS (1:9 v/v, pH 7.2, 0.066 M, Ar atmosphere), which are described below.

4.4.3. Incubation procedure for voltammetric studies

A 50 μM solution of **3a–c** in DMSO/PBS (1:9 v/v, pH 7.2, 0.066 M) was prepared and measured by means of CV technique. The same solutions were prepared by adding 25, 50, 75 and 100 μL mL^{-1} of dsDNA. After 45 min of incubation at 37 °C, the solution was purged with Ar in the electrochemical cell before each voltammetric measurement.

4.5. Computational details

The structures of the new quinones (**3a–c**), canonical nucleobases and two Watson-Crick H-bonded base pairs, namely adenineṡṡṡthymine (**A**···**T**) and guanineṡṡṡcytosine (**G**···**C**), together with the corresponding noncovalently bonded complexes formed between **3a-c** and both nucleobases models were fully optimized, by employing a dispersion-corrected meta-GGA exchange-correlation, TPSS-D3 (Tao, Perdew, Staroverov and Scuseria 2003; Grimme, Antony, Ehrlich and Krieg 2010), functional combined with a double-ζ quality 6-31 + G(d,p) basis set. Harmonic vibrational frequencies were computed in order to characterize them as minima on the potential energy surfaces. Two classes of noncovalently bonded complexes were found. The former is mainly stabilized by hydrogen-bonding type interactions while the second by π-π stacking type interactions. The stability of the intermolecular complexes was rationalized by the complexation energy (ΔE) that is calculated as follows:

$$\Delta E = E_{complex} - (E_{quinone} + E_{nucleobases}) \quad (3)$$

where $E_{complex}$, $E_{quinone}$ and $E_{nucleobases}$ correspond to the total electronic energy of the intermolecular complex, quinone **(3a–c),** and nucleobase models, respectively. All calculations were performed using the Gaussian09 suite of programs programs (Gaussian 03, 2004).

The reliability of the dispersion-corrected TPSS method is assured by the reasonably good results for the two planar Watson-Crick H-bonded base pairs, the computed interaction energies are −17.27 and −30.97 kcal/mol against −15.40 and −28.80 kcal/mol (Sponer, Jurecka and Hobza 2004), that are the best estimate for **A**···**T** and **G**···**C** pairs, respectively.

Acknowledgements

We gratefully acknowledge the financial support of FONDECYT (project 1161816) and the Millennium Nucleus of Chemical Processes and Catalysis (ICM - 120082). C. Espinosa-Bustos would like to thank FONDECYT (Postdoctoral fellowship 3150198).

References

Bard, A.J., Faulkner, L.R., 2000. Electrochemical Methods: Fundamentals and Applications. Wiley.

Asche, C., 2005. Antitumour quinones. Mini Rev. Med. Chem. 5, 449–467.

Bouffier, L., Gosse, I., Demeunynck, M., Mailley, P., 2012. Electrochemistry and bioactivity relationship of 6-substituted-4H-Pyrido [4,3,2-kl]acridin-4-one antitumor drug candidates. Bioelectrochemistry 88, 103–109.

Calderon-Arancibia, J., Espinosa-Bustos, C., Canete-Molina, A., Tapia, R.A., Faundez, M., Torres, M.J., Aguirre, A., Paulino, M., Salas, C.O., 2015. Synthesis and pharmacophore modelling of 2,6,9-trisubstituted purine derivatives and their potential role as apoptosis-inducing agents in cancer cell lines. Molecules 20, 6808–6826.

Cuellar, M.A., Salas, C., Cortes, M.J., Morello, A., Maya, J.D., Preite, M.D., 2003. Synthesis and in vitro trypanocide activity of several polycyclic drimane-quinone derivatives. Bioorg. Med. Chem. 11, 2489–2497.

Chaney, E.N., Baldwin, R.P., 1982. Electrochemical determination of adriamycin compounds in urine by pre-concentration at carbon paste electrodes. Anal. Chem. 54, 2556–2560.

Chen, X.X., Smith, G.D., Waring, P., 2003. Human cancer cell (Jurkat) killing by the cyanobacterial metabolite calothrixin A. J. Appl. Phycol. 15, 269–277.

Erdem, A., Ozsoz, M., 2002. Electrochemical DNA biosensors based on DNA-drug interactions. Electroanalysis 14, 965–974.

Ferreira Mdo, P., Cardoso, M.F., da Silva Fde, C., Ferreira, V.F., Lima, E.S., Souza, J.V., 2014. Antifungal activity of synthetic naphthoquinones against dermatophytes and opportunistic fungi: preliminary mechanism-of-action tests. Ann. Clin. Microbiol. Antimicrob. 13, 26.

Gaussian 03, Frisch, R.C., Trucks, M.J., Schlegel, G.W., Scuseria, H. B, Robb, G.E., Cheeseman, M.A., Montgomery, J.R., Jr., Vreven, J.A., Kudin, T., Burant, K.N, Millam, J. C., Iyengar, J.M., Tomasi, S.S., Barone, J., Mennucci, V., Cossi, B., Scalmani, M., Rega, G., Petersson, N., Nakatsuji, G.A., Hada, H., Ehara, M., Toyota, M., Fukuda, K., Hasegawa, R., Ishida, J., Nakajima, M., Honda, T., Kitao, Y., Nakai, O., Klene, H., Li, M., Knox, X., Hratchian, J.E., Cross, H.P., Bakken, J.B., Adamo, V., Jaramillo, C., Gomperts, J., Stratmann, R., Yazyev, R.E., Austin, O., Cammi, A.J., Pomelli, R., Ochterski, C., Ayala, J.W., Morokuma, P.Y., Voth, K., Salvador, G.A., Dannenberg, P., Zakrzewski, J.J., Dapprich, V.G., Daniels, S., Strain, A.D., Farkas, M.C. Malick, O., Rabuck, D.K., Raghavachari, A.D., Foresman, K., Ortiz,J.B., Cui,J.V., Baboul,Q., Clifford, A.G., Cioslowski,S., Stefanov, J., Liu, B.B., Liashenko, G., Piskorz, A., Komaromi, P., Martin, I., Fox, R.L., Keith, D.J., Al-Laham, T., Peng, M.A., Nanayakkara, C.Y., Challacombe, A., Gill, M., Johnson, P.M.W., Chen, B., Wong, M.W., Gonzalez, C., Pople, J.A. 2004. Gaussian, Inc., Wallingford CT.

Grimme, S., Antony, J., Ehrlich, S., Krieg, H. 2010. A consistent and accurate ab initio parametrization of density functional dispersion correction (DFT-D) for the 94 elements H-Pu. J. Chem. Phys. 132.

Guin, P.S., Das, S., Mandal, P.C., 2008. Electrochemical reduction of sodium 1,4-dihydroxy-9,10-anthraquinone-2-sulphonate in aqueous and aqueous dimethyl formamide mixed solvent: a cyclic voltammetric study. Int. J. Electrochem. Sci. 3, 1016–1028.

Guin, P.S., Das, S., Mandal, P.C., 2011. Electrochemical reduction of quinones in different media: a review. Int. J. Electrochem. 2011, 22.

He, P.X., Crooks, R.M., Faulkner, L.R., 1990. Adsorption and electrode-reactions of disulfonated anthraquinones at mercury-electrodes. J. Phys. Chem. 94, 1135–1141.

Hernandez, L.A., del Valle, M.A., Armijo, F., 2016. Electrosynthesis and characterization of nanostructured polyquinone for use in detection and quantification of naturally occurring dsDNA. Biosens. Bioelectron. 79, 280–287.

Hong, H.G., Park, W., 2001. Electrochemical characteristics of hydroquinone-terminated self-assembled monolayers on gold. Langmuir 17, 2485–2492.

Hong, Y., Sengupta, S., Hur, W., Sim, T., 2015. Identification of novel ROS inducers: quinone derivatives tethered to long hydrocarbon chains. J. Med. Chem. 58, 3739–3750.

Ibis, C., Tuyun, A.F., Ozsoy-Gunes, Z., Bahar, H., Stasevych, M.V., Musyanovych, R.Y., Komarovska-Porokhnyavets, O., Novikov, V., 2011. Synthesis and biological evaluation of novel nitrogen- and sulfur-containing hetero-1,4-naphthoquinones as potent antifungal and antibacterial agents. Eur. J. Med. Chem. 46, 5861–5867.

Kano, K., Konse, T., Nishimura, N., Kubota, T., 1984. Electrochemical properties of adriamycin adsorbed on a mercury-electrode surface. Bull. Chem. Soc. Jpn. 57, 2383–2390.

Klotz, L.O., Hou, X., Jacob, C., 2014. 1,4-naphthoquinones: from oxidative damage to cellular and inter-cellular signaling. Molecules 19, 14902–14918.

Kumagai, Y., Shinkai, Y., Miura, T., Cho, A.K., 2012. The chemical biology of naphthoquinones and its environmental implications. Annu. Rev. Pharmacol. Toxicol. 52, 221–247.

Maleev, V., Semenov, A., Kruglova, E., Bolbukh, T., Gasan, A., Bereznyak, E., Shestopalova, A., 2003. Spectroscopic and calorimetric study of DNA interaction with a new series of actinocin derivatives. J. Mol. Struct. 645, 145–158.

Mallavadhani, U.V., Prasad, C.V., Shrivastava, S., Naidu, V.G., 2014. Synthesis and anticancer activity of some novel 5,6-fused hybrids of juglone based 1,4-naphthoquinones. Eur. J. Med. Chem. 83, 84–91.

Martínez, M. J. A., Benito, P. B. 2005. Biological Activity of Quinones. Studies in Natural Products Chemistry. R. Atta ur, Elsevier. Vol. 30, 303–366.

Naujorks, A.A., da Silva, A.O., Lopes Rda, S., de Albuquerque, S., Beatriz, A., Marques, M.R., de Lima, D.P., 2015. Novel naphthoquinone derivatives and evaluation of their trypanocidal and leishmanicidal activities. Org. Biomol. Chem. 13, 428–437.

NCI 2014. NCI/NIH Developmental Therapeutics Program.

Ni, Y.N., Wang, Y.X., Kokot, S., 2011. Study of the interaction between 10-hydroxycamptothecine and DNA with the use of ethidiurn bromide dye as a fluorescence probe. Sens. Actuators B Chem. 156, 290–297.

Radi, A., El Ries, M.A., Kandil, S., 2005. Spectroscopic and voltammetric studies of Pefloxacin bound to calf thymus double-stranded DNA. Anal. Bioanal. Chem. 381, 451–455.

Radi, A.E., El-Naggar, A.E., Nassef, H.M., 2014. Electrochemical and spectral studies on the interaction of the antiparasitic drug nitazoxanide with DNA. Electrochim. Acta 129, 259–265.

Reisberg, S., Piro, B., Noel, V., Nguyen, T.D., Nielsen, P.E., Pham, M. C., 2008. Investigation of the charge effect on the electrochemical transduction in a quinone-based DNA sensor. Electrochim. Acta 54, 346–351.

Ryvolova, M., Adam, V., Eckschlager, T., Stiborova, M., Kizek, R., 2012. Study of DNA-ellipticine interaction by capillary electrophoresis with laser-induced fluorescence detection. Electrophoresis 33, 1545–1549.

Salas, C.O., Faundez, M., Morello, A., Maya, J.D., Tapia, R.A., 2011. Natural and synthetic naphthoquinones active against Trypanosoma cruzi: an initial step towards new drugs for Chagas disease. Curr. Med. Chem. 18, 144–161.

Sieveking, I., Thomas, P., Estevez, J.C., Quinones, N., Cuellar, M.A., Villena, J., Espinosa-Bustos, C., Fierro, A., Tapia, R.A., Maya, J. D., Lopez-Munoz, R., Cassels, B.K., Estevez, R.J., Salas, C.O., 2014. 2-Phenylaminonaphthoquinones and related compounds: synthesis, trypanocidal and cytotoxic activities. Bioorg. Med. Chem. 22, 4609–4620.

Smith, N.A., Byl, J.A.W., Mercer, S.L., Deweese, J.E., Osheroff, N., 2014. Etoposide quinone is a covalent poison of human topoisomerase IIβ. Biochemistry 53, 3229–3236.

Sponer, J., Jurecka, P., Hobza, P., 2004. Accurate interaction energies of hydrogen-bonded nucleic acid base pairs. J. Am. Chem. Soc. 126, 10142–10151.

Stanicova, J., Fabriciova, G., Chinsky, L., Sutiak, V., Miskovsky, P., 1999. Amantadine-DNA interaction as studied by classical and resonance Raman spectroscopy. J. Mol. Struct. 478, 129–138.

Tanaka, H., Aramata, A., 1997. Aminopyridyl cation radical method for bridging between metal complex and glassy carbon: cobalt(II) tetraphenylporphyrin bonded on glassy carbon for enhancement of CO_2 electroreduction. J. Electroanal. Chem. 437, 29–35.

Tandon, V.K., Kumar, S., 2013. Recent development on naphthoquinone derivatives and their therapeutic applications as anticancer agents. Expert Opin. Ther. Pat. 23, 1087–1108.

Tandon, V.K., Maurya, H.K., Tripathi, A., ShivaKeshava, G.B., Shukla, P.K., Srivastava, P., Panda, D., 2009. 2,3-Disubstituted-1,4-naphthoquinones, 12H-benzo[b]phenothiazine-6,11-diones and related compounds: synthesis and biological evaluation as potential antiproliferative and antifungal agents. Eur. J. Med. Chem. 44, 1086–1092.

Tandon, V.K., Maurya, H.K., Yadav, D.B., Tripathi, A., Kumar, M., Shukla, P.K., 2006a. Naphtho[2,3-b][1,4]-thiazine-5,10-diones and 3-substituted-1,4-dioxo-1,4-dihydronaphthalen-2-yl-thioalkanoate derivatives: synthesis and biological evaluation as potential antibacterial and antifungal agents. Bioorg. Med. Chem. Lett. 16, 5883–5887.

Tandon, V.K., Yadav, D.B., Maurya, H.K., Chaturvedi, A.K., Shukla, P.K., 2006b. Design, synthesis, and biological evaluation of 1,2,3-trisubstituted-1,4-dihydrobenzo[g]quinoxaline-5,10-diones and related compounds as antifungal and antibacterial agents. Bioorg. Med. Chem. 14, 6120–6126.

Tao, J. M., Perdew, J. P., Staroverov, V. N., Scuseria, G. E. 2003. Climbing the density functional ladder: Nonempirical meta-generalized gradient approximation designed for molecules and solids. Phys. Rev. Lett. 91.

Please cite this article in press as: Espinosa-Bustos, C. et al., Unveiling interactions between DNA and cytotoxic 2-arylpiperidinyl-1,4-naphthoquinone derivatives: A combined electrochemical and computational study. Arabian Journal of Chemistry (2018), https://doi.org/10.1016/j.arabjc.2018.04.008

Tip-pyang, S., Limpipatwattana, Y., Khumkratok, S., Siripong, P., Sichaem, J., 2010. A new cytotoxic 1-azaanthraquinone from the stems of Goniothalamus laoticus. Fitoterapia 81, 894–896.

Vazquez, K., Espinosa-Bustos, C., Soto-Delgado, J., Tapia, R.A., Varela, J., Birriel, E., Segura, R., Pizarro, J., Cerecetto, H., Gonzalez, M., Paulino, M., Salas, C.O., 2015. New aryloxy-quinone derivatives as potential antiChagasic agents: synthesis, trypanosomicidal activity, electrochemical properties, pharmacophore elucidation and 3D-QSAR analysis. Rsc Adv. 5, 65153–65166.

Wellington, K.W., 2015. Understanding cancer and the anticancer activities of naphthoquinones – a review. Rsc Adv. 5, 20309–20338.

Zhou, J., Duan, L., Chen, H.M., Ren, X.M., Zhang, Z., Zhou, F.T., Liu, J.S., Pei, D.Q., Ding, K., 2009. Atovaquone derivatives as potent cytotoxic and apoptosis inducing agents. Bioorg. Med. Chem. Lett. 19, 5091–5094.

Please cite this article in press as: Espinosa-Bustos, C. et al., Unveiling interactions between DNA and cytotoxic 2-arylpiperidinyl-1,4-naphthoquinone derivatives: A combined electrochemical and computational study. Arabian Journal of Chemistry (2018), https://doi.org/10.1016/j.arabjc.2018.04.008